*Paper No. 390. (quote when citing this article)*
Eleventh World Conference on Earthquake Engineering
ISBN: 0 08 042822 3

# EVALUATION OF A COUNTERMEASURE AGAINST LIQUEFACTION FOR OIL TANK SITE

JINGZHE ZHENG and NAOTO OHBO

Civil Engineering Department I, Kajima Technical Institute, Kajima Corporation,
19-1, Tobitakyu 2-Chome, Chofu-shi, Tokyo 182, Japan

## ABSTRACT

This paper evaluates a countermeasure against liquefaction for oil tank site through simulation of earthquake observation and numerical liquefaction analysis assuming large earthquakes. The countermeasure is to use a sheet pile ring to constrain the soil under oil tank. The simulation of earthquake responses observed at tank sites with and without sheet pile-ring is first performed to validate a 3D finite element numerical model. Using the numerical model, liquefaction analysis during large earthquakes is performed, and the excess pore water pressure generated in the soil and the settlement of tank are investigated. The results show that the presented numerical model could simulate the observed earthquake responses of tank-ring-soil system, and that the excess pore water pressure and the settlement of the tank could be significantly reduced using a sheet pile ring.

## KEYWORDS

Oil tank; liquefaction; countermeasure; earthquake observation; 3D FEM; 2-phase nonlinear analysis.

## INTRODUCTION

The investigation of the damage due to earthquakes (e.g., JSCE, 1986) has revealed that soil liquefaction may cause severe damage to oil storage tank. Therefore, to develop countermeasures against liquefaction has become an urgent task. During these years, several countermeasures against liquefaction for tank sites have been proposed based on the lessons learnt from the past earthquake damage (e.g., JSSMFE, 1993). One of the promising methods is the sheet pile ring countermeasure (Sawauchi *et al.*, 1991), which is to constrain the soft soil under tank by a sheet pile ring inserting into hard underlying soil.

This study attempts to evaluate the sheet pile ring countermeasure for tank sites through 3D 2-phase nonlinear finite element analysis. The liquefaction analysis code DYNAFLOW (Prevost, 1981) is adopted as analysis tool. A 3D finite element model of tank-ring-soil system is first established, and the simulation of the results of earthquake observations (Ohbo *et al.*, 1992), which are conducted at oil tank sites with and without sheet pile-ring, is performed to verify the numerical model. Using the validated numerical model, the performance of the countermeasure is evaluated through numerical simulation assuming large earthquake.

## COUNTERMEASURE AND OBSERVATION

Figure 1 demonstrates the outline of the sheet pile ring countermeasure. The soil under tank is constrained by a sheet pile ring, which inserts into the hard underlying soil. The expected functions of the countermeasure are as following: (a)to mitigate the shear deformation of the soil, and reduce the excess pore water pressure in the

soil under and around tank ; and (b) to prevent large lateral deformation of soil even if liquefaction occurs, and reduce the magnitude of settlement of tank.

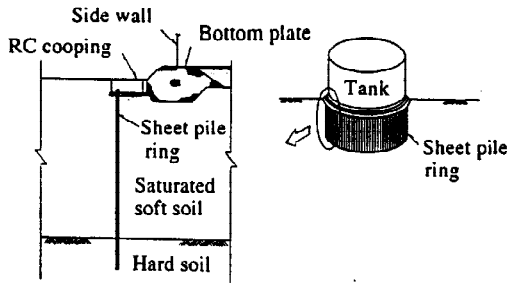


Fig. 1. Outline of countermeasure.

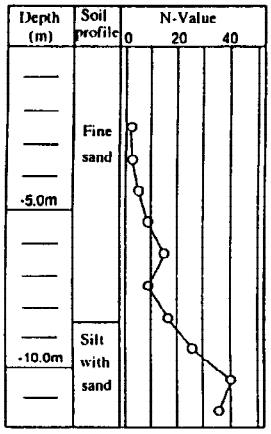


Fig. 2. Soil profile at observation site.

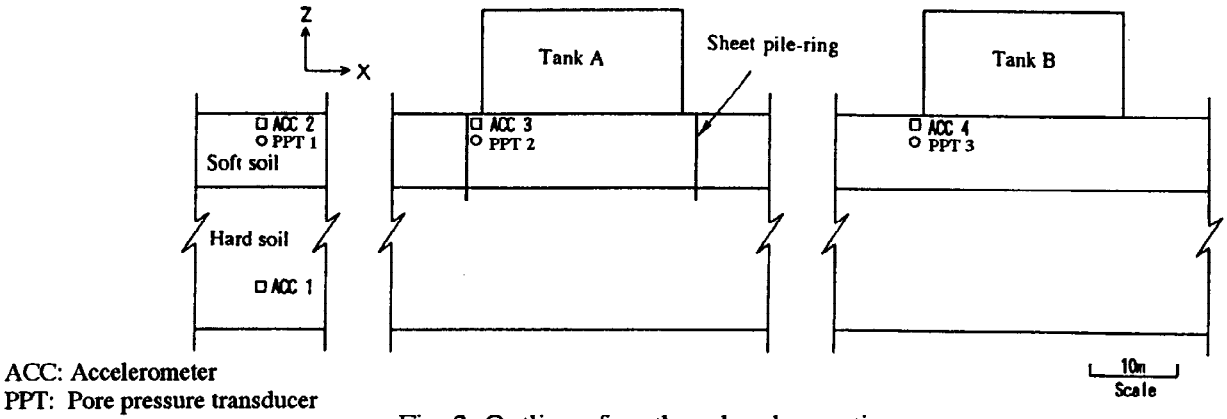


Fig. 3. Outline of earthquake observation.

In order to confirm the performance of the sheet pile ring countermeasure, earthquake observation has been conducted for the cases with and without the countermeasure since 1991 (Ohbo *et al.*, 1992). The observation site is located in the Tokyo bay. Boring test and P-S logging have been conducted at the site, and conventional laboratory soil tests together with liquefaction strength tests also performed. Figure 2 shows the soil profile. A soft saturated layer with thickness of 8.5m is based on a hard soil. Figure 3 represents the actual tank-sheet pile ring-soil system together with the arrangement of accelerometers and excess pore water pressure transducers. The diameter of the tanks D is 23.42m, and the height of oil is 11.79m. The steel sheet pile ring with depth of 10m inserts into hard soil layer by 1.5m. The thickness of the sheet pile is 0.013m (YSP-FA), and the Young modulus is 205,800Mpa.

Up to now, more than 40 earthquakes have been recorded. The largest acceleration response and pore pressure were observed during the earthquake called Tokyo-Bay-Earthquake, which occurred on February 2, 1992. The magnitude of the earthquake is 5.9, and the focal depth and epicentral distance are 93km and 33km, respectively. The observed results during this earthquake are chosen for simulation. Figure 4 indicates the observed accelerations during the earthquake. The accelerations show large amplitudes from about 2.4 seconds, and begin to decrease about 1 seconds later. The maximum acceleration of 1.59m/s$^2$ is observed at GL-1m in free-field. The smallest acceleration is at GL-20m in free-field, which has amplitude of 0.89m/s$^2$. The maximum accelerations at GL-1m under tank A (with sheet-pile-ring) and B (without ring) are 0.96 m/s$^2$ and 1.26 m/s$^2$, respectively, representing that the sheet pile ring reduced the amplitude during this earthquake. Figure 5 summaries the observed excess pore water pressures. Excess pore water pressure increases as acceleration approaches peak value, and soon reach its maximum, and then gradually dissipate as acceleration decreases with time. The maximum excess pore water pressure at GL-3m under tank A and B are 5.27kPa and 6.90kPa, respectively, indicating that the use of a sheet pile ring leads to small amplitude of excess pore water pressure. The maximum excess pore water pressure ratio, which is defined as the ratio between the excess pore water pressure and the initial vertical effective stress, is found at GL-3m in free-field, which has value of 0.145.

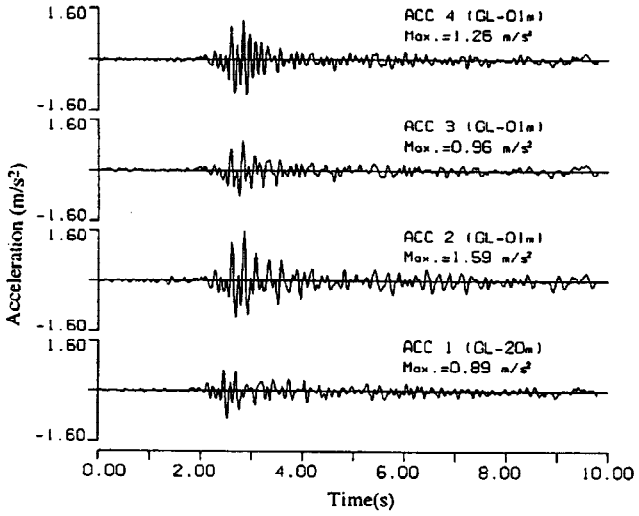


Fig. 4. Observed accelerations.

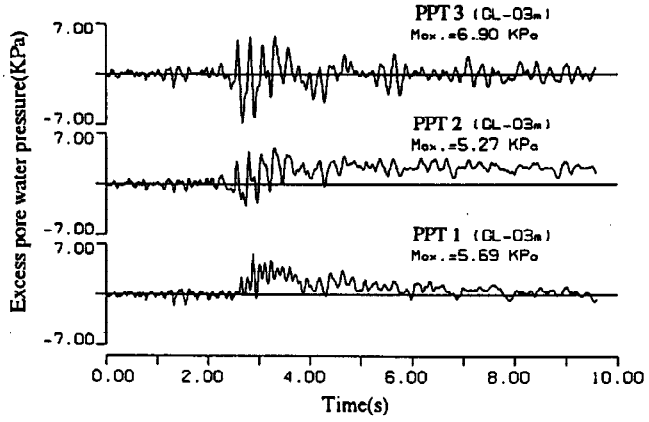


Fig. 5. Observed excess pore water pressures.

## FINITE ELEMENT MODEL

The computer code used for numerical analysis is DYNAFLOW (Prevost, 1981; last update 1994), which is a finite element analysis program designed to perform nonlinear seismic response calculations. Dry, saturated and partially saturated soils can be analyzed. The solid and fluid coupled filed equations and constitutive equations are general and applicable to three dimensional situations. Figure 6 shows the 3D finite element model of oil tank-sheet pile ring-soil system.

The upper soft saturated soil is modeled as nonlinear 2-phase material (Vs=100m/s), and underlying hard soil linear single phase one (Vs=400m/s). The multi-yield constitutive soil model (Prevost, 1985) is selected to simulate the nonlinear behavior of the soil materials. In this study, mass density and porosity are determined from the results of routine soil tests. Initial elastic shear modulus are obtained from shear wave velocity and mass density, and bulk modulus computed assuming poisson's ratio as 0.3. The reference mean normal stress is selected as 40kPa, and power exponent 0.5. Friction angle at failure is determined from N value, using the correlation equation suggested by Dunhum (JSSMFE, 1982). Maximum deviatoric strain and dilation angle are determined referring to the results of similar soil (JSSMFE, 1979). Dilation parameter ($X_{pp}$) is evaluated by fitting the liquefaction strength curve as shown in Fig. 7. The coefficient of permeability is determined according to Akai's classification (JSSMFE, 1982). Table 1 shows the determined material parameters. In 3D finite element model, soil is represented by eight-node elements with 6 degrees of freedom node (three for solid

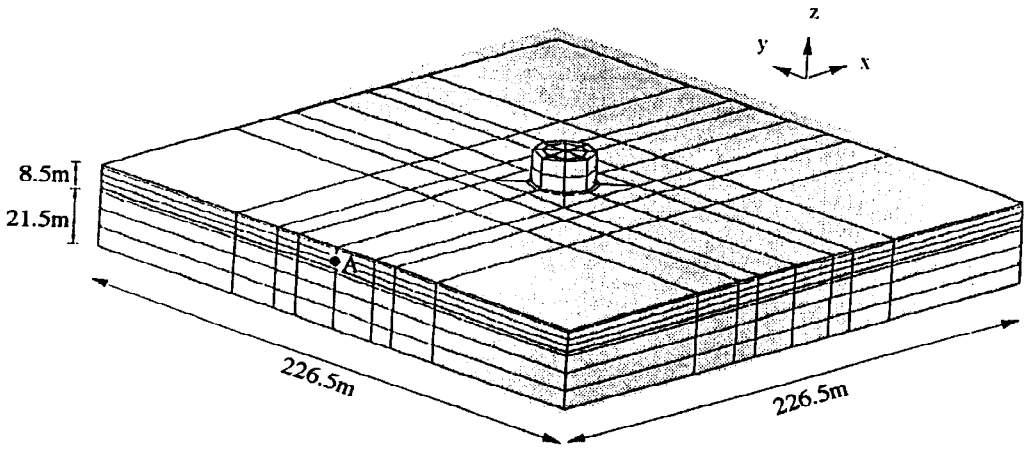


Fig. 6. 3D finite element model of tank-ring-soil system.

phase displacements and three for water) for upper soil and 3 degrees of freedom for lower layer. The base is assumed rigid, and acceleration wave is applied to the horizontal degree of freedom at the base. Vertical degree of freedom at the base is fixed. The lateral soil boundaries are set far from the edge of tank, and is taken as free-field. The nodes at lateral boundary of soils at the same depth are tied so that they have the same displacement all the time. Sheet pile ring is modeled using four-node shell element. At vertical sand-ring interface, it is assumed that there is no friction.

As for the modeling of oil-tank system, several approaches have been proposed. Veletsos *et al.* (1992) have conducted a series of studies on dynamic response of liquid-tank-soil system, and pointed out that the single-degree-of-freedom approximation would be quite adequate for relatively broad tanks with height-to-radius ratios of the order of 1.5 or less. The height-to-radius ratio of the tank investigated here is 1.02, and it may be estimated a model which has the same fundamental period as that of oil-tank system obtained by rigorous method, could approximately represent the dynamic behavior of oil-tank system. Yokoyama *et al.* (1988) simulated the observed acceleration response of liquid-tank-soil system using 3D finite element model. In their model, liquid is represented by solid elements with the same mass density as liquid, and the Young's modulus is so determined that the fundamental period of the model using solid element is the same as that of actual liquid-tank system. Their computed results well agreed with the observed ones. Taking the above into account, in this study, oil-tank system is represented by eight-node solid elements, whose mass density and Young's modulus are determined using the method suggested by Yokoyama. The fundamental period of oil-tank system is calculated using the approach proposed by Sakai *et al.* (1988). The computed fundamental period of oil-tank system under investigation is 0.156s.

The calculation is performed in two steps. First, consolidation under gravity loads is calculated. After consolidation is completed, the nodal displacement, velocity and acceleration are cleared to zero, and acceleration is input from the base. The Newmark parameters in the integration scheme are chosen as r=0.65 and $\beta=(r+0.5)^2/4=0.33$.

Table 1. Parameters for saturated soil

| Property | Value |
|---|---|
| Mass density - solid | 2699.0 kg/m$^3$ |
| Porosity | 0.448 |
| Initial shear modulus | 18.0 Mpa |
| Initial bulk modulus | 39.0 Mpa |
| Reference mean effective normal stress | 40.0 kPa |
| Power exponent | 0.5 |
| Friction angel at failure | 38.0 deg. |
| Cohesion | 0 |
| Maximum deviatoric strain(compression / extension) | 6.0/5.0 % |
| Dilation angle | 30.0 |
| Dilation parameter | 0.09 |
| Permeability | 1.0E-05 m/s |

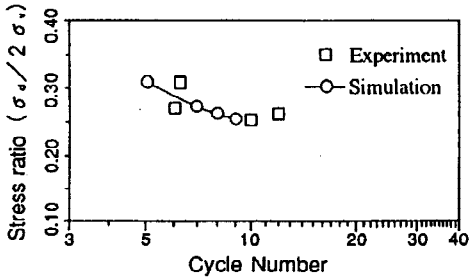


Fig. 7. Liquefaction strength curve

## EVALUATION OF COUNTERMEASURE

### Simulation of earthquake observation

The records during Tokyo-Bay-Earthquake described before have been simulated. The input acceleration wave at GL-30m is computed using the acceleration waves observed at GL-20m by 1D equivalent linear analysis. Figure 8 shows the input acceleration. Only horizontal input is considered.

The computed and observed acceleration responses at GL-1m and excess pore water pressures at GL-3m in free-filed are indicated in Fig. 9. Calculated results match observed ones very well, although observed excess pore water pressure show some oscillation which may result from the effects of vertical motion. Figure 10 compares the computed and recorded acceleration responses at GL-1m under tank for the cases with and without sheet pile ring. The computed results agree well with the recorded ones in both cases. The computed and recorded excess pore water pressures at GL-3m under tank are compared in Fig. 11. Fair agreement is reached. In the case with sheet pile ring, observed excess pore water pressure dissipates slowly compared with the computed one. The difference may come from the local soil condition around the pore pressure transducer in the case with sheet pile ring.

From the comparison between computed and observed results shown above, it could be concluded that the FEM model constructed here is able of representing the main features of the earthquake response of actual tank-ring-oil system.

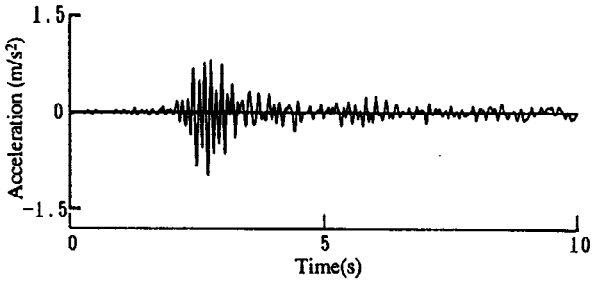


Fig. 8. Input wave for simulation of earthquake observation

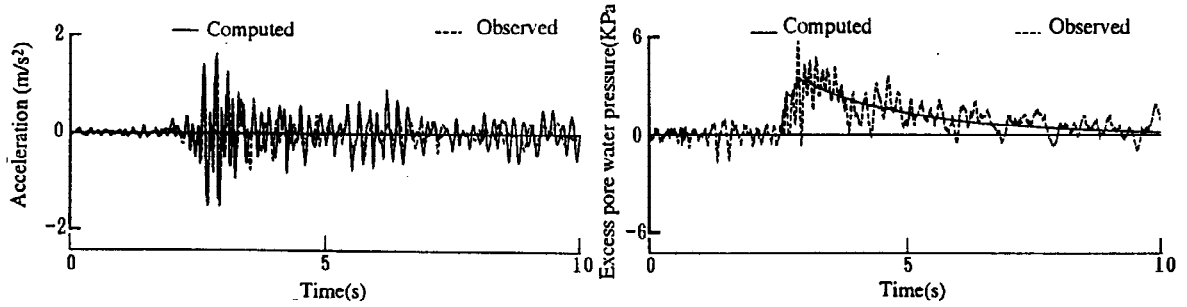


Fig. 9. Computed and observed accelerations and excess pore water pressures (free-field).

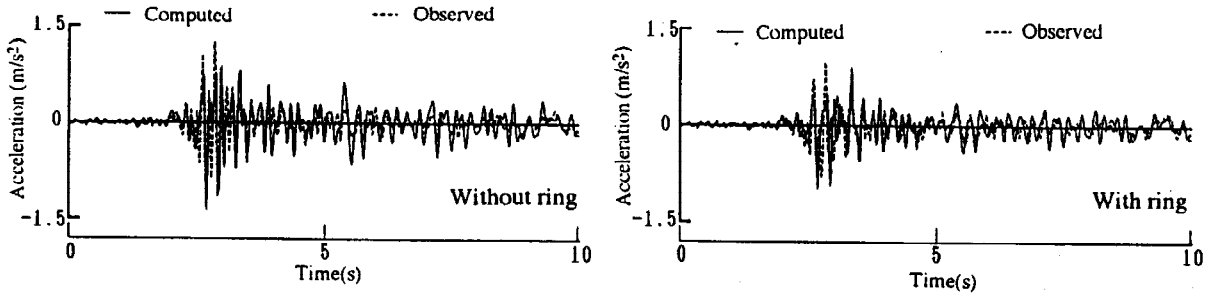


Fig. 10. Computed and observed accelerations (under tank).

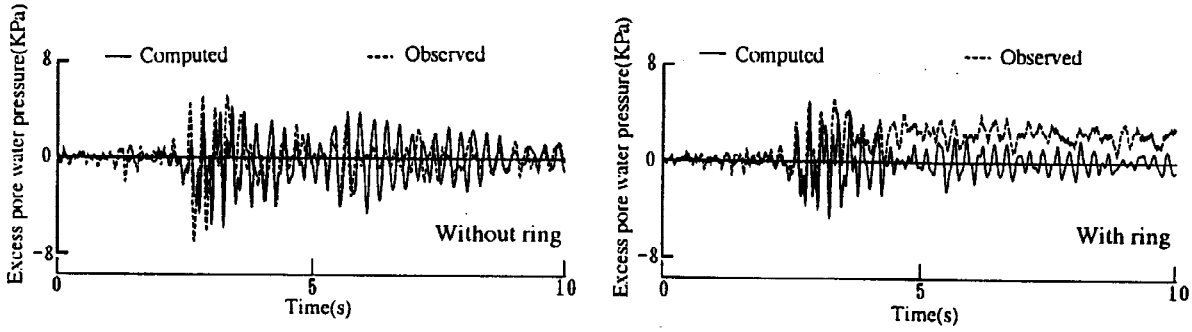


Fig. 11. Computed and observed excess pore water pressures (under tank).

Liquefaction analysis

In order to evaluate the performance of the sheet pile ring countermeasure, liquefaction simulation is performed by applying acceleration of large amplitude at the base in x direction. El Centro NS wave is adopted as input. The maximum amplitude of input wave is scaled to 2.0m/s$^2$. Figure 12 shows the input wave.

The time histories of acceleration response and excess pore water pressure ratio at point A at lateral boundary (see Fig. 6) are shown in Fig. 13. The excess pore water pressure ratio develops when acceleration increases, and reaches to 0.9 at around 2.8 seconds, from which it is confirmed that the soil almost liquefies. The time

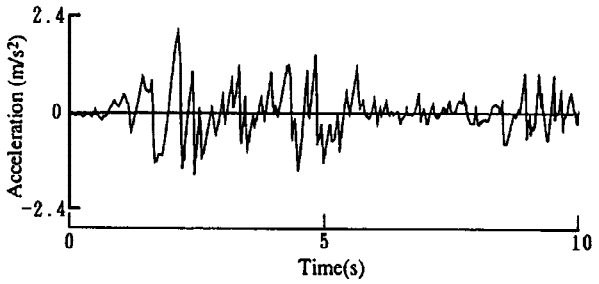


Fig. 12. Input wave for liquefaction simulation.

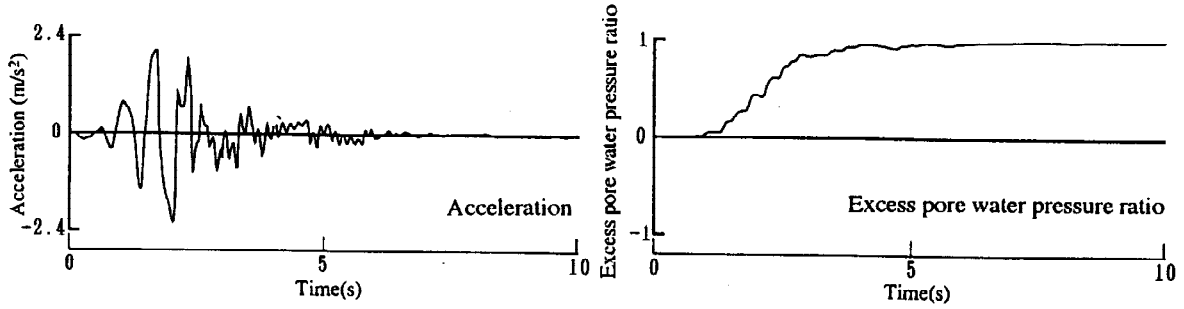


Fig. 13. Acceleration and excess pore water pressure ratio at point A (free-field).

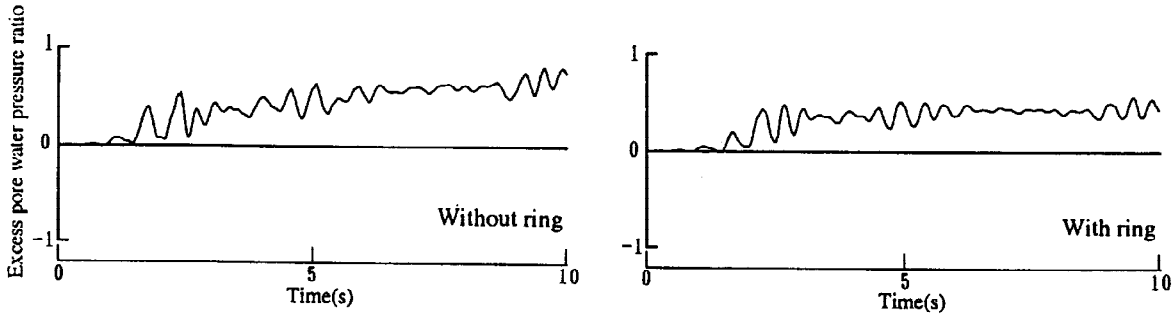


Fig. 14. Excess pore water pressure ratio at a point under tank center (GL-3.5m).

history of excess pore water pressure ratio at a point beneath the center of tank with depth of 3.5m are shown in Fig. 14. The excess pore water pressure ratio in both cases are smaller than that at point A, indicating that the soil under tank is harder to liquefy compared with the soil in free-field. Compared with the case without sheet pile-ring, the excess pore water pressure ratio in the case with sheet pile ring demonstrates smaller value. Figure 15 shows the distributions of excess pore water pressure ratio at the end of shaking. In the case without sheet pile ring, the region in which excess pore water pressure ratio is larger than 0.8 extends to the place about 0.24D from the edge of tank. The maximum excess pore water pressure ratio in the soil under tank is bigger than 0.6, demonstrating a significant reduction of soil strength. On the other hand, in the case with sheet pile ring, the region with excess pore water pressure ratio greater than 0.8 significantly decreases, which is about 0.7-1.26D from the edge of tank. The maximum excess pore water pressure ratio in the soil beneath the center of tank is less than that observed in the case without sheet pile ring. It is interesting to note that sheet pile ring reduce the excess pore water pressure in the soil not only inside the ring but also outside the ring to a quite distance. The tank settlement during shaking is represented in Fig. 16. It can be seen that using a sheet pile ring reduces the settlement of tank by 90%, which clearly reflects the effects of the sheet pile ring. Figure 17 represents the deformation of tank and soil beneath the tank. In the case without ring, the soil beneath tank horizontally deforms towards the liquefied region due to the weight of tank, which results in large settlement of tank. On the other hand, in case with ring, the deformation of soil beneath tank is constrained by the ring to a very small magnitude, although the soil outside the ring liquefies. From the above results, it could be concluded that tank settlement comes from the horizontal deformation of underlying soil which results from the liquefaction of surrounding soil, and the use of sheet pile ring could well constrain the horizontal deformation of inside soil, and thus significantly reduce the settlement of tank.

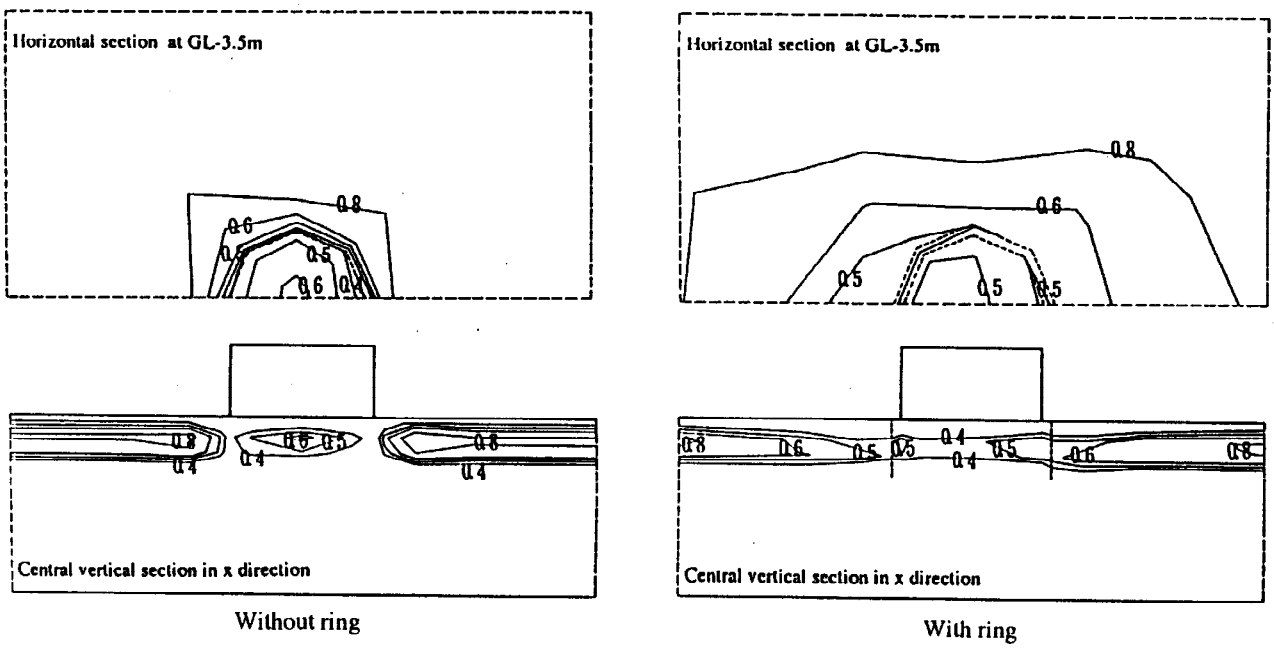


Fig. 15. Distribution of excess pore water pressure ratio at end of shaking.

The investigation on the effects of two horizontal direction input has also been performed by applying the acceleration wave shown in Fig. 12 in x direction, and El Centro EW wave in y direction at the base. The maximum amplitude of input wave in y direction is also 2.0m/s$^2$. It is confirmed that, even in the case with sheet pile ring, the excess pore water pressure ratio in the soil under tank reaches to 0.8. The settlement of tank is shown in Fig. 16. Compared with the results of the case with one direction input, the settlement in the case with two horizontal direction input increases by 50%. The results of the excess pore water pressure ratio and the settlement of tank demonstrate the necessity to consider the effects of two direction input when the input waves in two directions are both large. It should be mentioned that even in the case with two direction input, the use of a sheet pile ring could limit the settlement of tank to a very low magnitude.

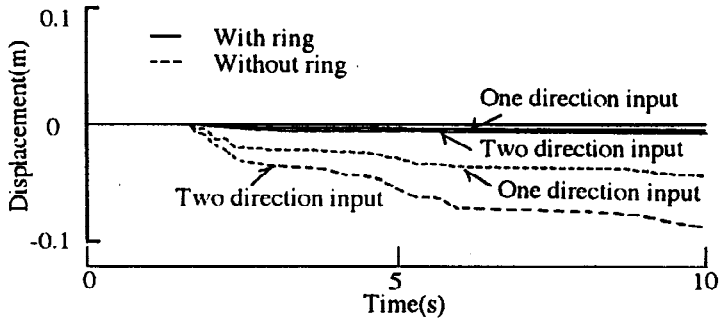


Fig. 16. Settlement of tank

## CONCLUSIONS

In order to evaluate the sheet pile ring countermeasure against liquefaction for tank site, a 3D finite element model of tank-sheet pile ring-soil system is constructed, and validated through the simulation of earthquake observation. Using the validated model, 2-phase nonlinear earthquake response analysis is conducted to evaluate the countermeasure assuming large earthquake. Main conclusions drawn from this study are as following; (1) The presented 3D finite element model could simulate the acceleration responses and excess pore water pressures observed at oil tank sites during earthquakes; (2) The use of a sheet pile ring reduce the excess pore water pressure generated in the soil under and around tank, and remarkably reduce the settlement of tank during large earthquakes; and (3) Compared with one horizontal direction input, two horizontal direction input causes larger excess pore water pressure in the soil, and increases the settlement of tank.

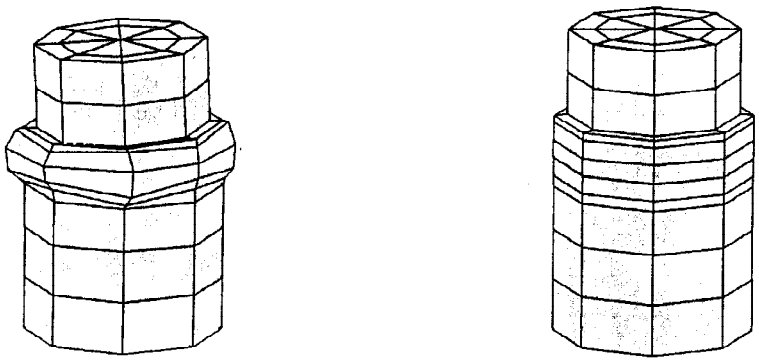

Without ring

With ring

Fig. 17. Deformation of soil beneath tank at end of shaking.

REFERENCE


Bouckovalas, G.,Stamatopoulos, C.A. and R.V. Whitman (1991). Analysis of settlements and pore pressures in centrifuge tests, *Journal of Geotechnical Engineering,* ASCE, **117**(10), 1492-1508.

JSCE(1986). *Damage report of the Nihon-kai Central Part Earthquake in 1983.* JSCE, Tokyo. (in Japanese)

JSSMFE (1979).*Methods of Soil Tests.* JSSMFE, Tokyo. (in Japanese)

JSSMFE (1982). *Handbook of Soil Engineering.* JSSMFE, Tokyo. (in Japanese)

JSSMFE (1993). Countermeasures against soil liquefaction. JSSMFE, Tokyo. (in Japanese)

Ohbo, N., Sawauchi, T. and H. Hayashi (1992). Earthquake observation at a tank site reinforced by a sheet pile-ring. Proc. 48th annual convention of JSCE, 392-393. (in Japanese)

Prevost, H.J.(1981). DYNAFLOW: A nonlinear transient finite element analysis program. Dept. Civil Engrg. Op. Res., Princeton University. Last update 1994.

Prevost, H.J. (1985). A simple plasticity theory for frictional cohensionless soils. *J. Soil Dynam. Earthq. Eng.*. **4**(1), 9-17.

Sakai, F., Ogawa, H. and A.Isoe (1988). Horizontal, vertical and rocking fluid-elastic response and design of cylindrical liquid storage tanks. Proc. of 8WCEE, Vol. VII, 263-270.

Sawauchi, Y., Suzuki, K., Hamada, T., Aoyagi, T. and N. Ando (1991). A countermeasure against liquefaction for oil storage tank site. Proc. 47th annual convention of JSCE, 280-281. (in Japanese)

Veletsos, A.S., Tang, Y. and H.T. Tang (1992). Dynamic response of flexibly supported liquid-storage tanks. *J. Struct. Engrg. Div.*, ASCE, **118**(1), 264-283.

Yokoyama, M., Murano, M. and S. Nishihashi (1988). Earthquake observation and coupled vibrational analysis of cylindrical water storage tank. Proc. of 8WCEE, Vol. VII, 389-396.